Stable magnetization states under a spin-polarized current and a magnetic field

Hirofumi Morise* and Shiho Nakamura
Corporate R&D Center, Toshiba Corporation, Saiwai-ku, Kawasaki 212-8582, Japan
(Received 10 August 2004; revised manuscript received 5 November 2004; published 28 January 2005)

Stable magnetization states of a nanoscale magnet under torque by a spin-polarized current and one under torque by an external magnetic field are studied theoretically. We consider six configurations for the combination of the three directions, that is, the easy axis of the magnet, the spin polarization of the current, and the magnetic field. For each configuration, all the possible stable magnetization states are revealed by constructing a phase diagram in the current-field plane on the basis of the Landau-Lifshitz-Gilbert equation. In addition, analyses on the dynamic behaviors of the magnetization are presented. We find that our system does not exhibit any chaotic behaviors. Nevertheless, the initial condition has a significant effect on the magnetization motion.

DOI: 10.1103/PhysRevB.71.014439 PACS number(s): 75.75.+a, 72.25.Ba, 75.60.Jk

I. INTRODUCTION

The concept of the "spin-transfer torque" proposed by Slonczewski[1] and Berger[2] offers a new way of controlling the magnetization, which replaces the conventional method utilizing magnetic fields. The transfer of the spin angular momentum between two magnetic layers by the current-perpendicular-to-plane can reverse the magnetization of one of the magnetic layers.[3–9] The technology utilizing the spin-transfer torque is expected to increase the recording density of the magnetoresistive random access memories (MRAMs) and other data storage devices.

One of the attractive topics related to this subject is the magnetization under coexistence of the spin-transfer torque and the magnetic field. Early theoretical works[1,5,10] derived an analytical expression for the critical reversal current, which includes the effect of a rather small magnetic field, which is typically less than the coercive field. Later, the critical current for a larger magnetic field was also obtained.[11,12] Furthermore, the existence of new equilibrium states and of the nondecaying precessional states is also pointed out.[11,13] These stable states are characteristic features of the magnetization under the spin-polarized current and the magnetic field. An experimental confirmation of the precessional motion is reported in Ref. 14.

The aim of the present work is twofold. First, we reveal all the possible equilibrium states of the magnetization and their stability conditions in the whole ranges of the spin-polarized current and the magnetic field. We employ the macrospin model and the Landau-Lifshitz-Gilbert (LLG) equation, which has been used mostly for the investigation of fundamental behaviors of the magnetization. The assumption of the coherent rotation of the magnetization, which the macrospin model is based on, is known to be valid with respect to the properties of the equilibrium magnetization state for a small enough magnet.[11] Furthermore, this model enables an analytical calculation, and therefore, is suitable for exhaustive studies. We investigate totally six configurations of the combination of the three directions, that is, the easy axis of the magnet, the spin polarization of the current, and the magnetic field. We construct a phase diagram for each case.

Second, we consider dynamic behaviors of the magnetization for some cases on the basis of the fully time-dependent LLG equation. This clarifies the details of the magnetization dynamics which is beyond the linearly oscillating regime.

The present work is organized as follows. In Sec. II, the LLG equation which dictates the dynamic behavior of the macrospin is introduced. We consider the equilibrium states and their linear stability. In Sec. III, the phase diagram is constructed. In Sec. IV, we pick up some cases and discuss the dynamic behaviors of the magnetization. Section V is devoted to conclusions.

II. FORMULATION

We consider a system composed of two ferromagnetic layers separated by a nonmagnetic layer. When the current in the direction perpendicular to the plane is introduced, the magnetization of the thinner (free) magnetic layer receives torques from the current which is polarized in the direction of the magnetization of the thicker (pinned) layer $\hat{\boldsymbol{m}}_{\mathrm{pin}}$. The dynamic behavior of the magnetization of the free layer $\boldsymbol{M}$ is governed by the following LLG equation:[1]

$$\frac{d\boldsymbol{M}}{dt} = -\frac{\alpha}{M}\boldsymbol{M}\times\frac{d\boldsymbol{M}}{dt} - \gamma\boldsymbol{M}\times\frac{\partial E}{\partial \boldsymbol{M}} + \frac{2\mu_B}{VM^2}\frac{gI_e}{|e|}\boldsymbol{M} \times (\hat{\boldsymbol{m}}_{\mathrm{pin}}\times\boldsymbol{M}). \tag{1}$$

Here, the first term in the right-hand side, including the Gilbert constant α, denotes the decaying term. M is the saturation magnetization. The second term, including the gyromagnetic ratio γ, denotes the coupling with the effective magnetic field $-\partial E/\partial \boldsymbol{M}$. Here, E is the magnetic energy, which is a summation of the anisotropy energy and the coupling one with the external field $\boldsymbol{H}_{\mathrm{ext}}$:

$$E = E_{\mathrm{an}} + E_{\mathrm{ext}}, \tag{2}$$

$$E_{\mathrm{an}} = \frac{H_K}{2M}[M^2 - (\boldsymbol{M}\cdot\hat{\boldsymbol{c}})^2] - 2\pi[M^2 - (\boldsymbol{M}\cdot\hat{\boldsymbol{n}})^2], \tag{3}$$

$$E_{\mathrm{ext}} = -\boldsymbol{M}\cdot\boldsymbol{H}_{\mathrm{ext}}. \tag{4}$$

The first term in E_{an} (3) denotes the uniaxial anisotropy along the unit vector $\hat{\boldsymbol{c}}$. H_K indicates its effective field. The

second term denotes the anisotropy of easy-plane whose unit normal vector is $\hat{\boldsymbol{n}}$.

The third term in the right-hand side of Eq. (1) denotes the spin-transfer torque driven by the current injection. $\hat{\boldsymbol{m}}_{\rm pin}$ is the unit vector in the direction of the magnetization of the pinned layer, and therefore the direction of the spin polarization of the introduced current. μ_B and V are Bohr magneton and the volume, respectively. The factor g represents the "efficiency."[1]

We introduce the dimensionless quantities here

$$\hat{\boldsymbol{m}} \equiv \frac{\boldsymbol{M}}{M}, \quad \tau \equiv \frac{2\pi M \gamma t}{1+\alpha^2}, \quad j \equiv \frac{\hbar}{2\pi M^2 V}\frac{g I_e}{|e|},$$

$$\tilde{\boldsymbol{h}} \equiv -\frac{1}{2\pi M}\frac{\partial E}{\partial \boldsymbol{M}} + j\hat{\boldsymbol{m}}_{\rm pin} \times \hat{\boldsymbol{m}}. \tag{5}$$

In terms of these symbols, the LLG equation (1) is rewritten as

$$\dot{\hat{\boldsymbol{m}}} = \alpha \tilde{\boldsymbol{h}}_\perp + \hat{\boldsymbol{m}} \times \tilde{\boldsymbol{h}}_\perp, \tag{6}$$

where $\tilde{\boldsymbol{h}}_\perp \equiv \tilde{\boldsymbol{h}} - (\tilde{\boldsymbol{h}} \cdot \hat{\boldsymbol{m}})\hat{\boldsymbol{m}}$, and the overdot denotes the derivative with the scaled time τ.

Here, we briefly summarize the linear analysis, which is used in the following sections. The unit vector $\hat{\boldsymbol{m}}$ can be expressed as a function of two variables, symbolically denoted by x_1 and x_2. We can rewrite the LLG equation (6) in the form

$$\dot{x}_i = f_i(x_1, x_2) \quad (i = 1, 2). \tag{7}$$

The equilibrium state is defined as the state corresponding to the solution of $f_1 = f_2 = 0$. The linear stability of the equilibrium state is given by the condition that all eigenvalues of the matrix $L = (L_{ij}) \equiv (\partial f_i / \partial x_j)$ have negative real parts. This condition is reduced to $\mathrm{tr}\, L < 0$ and $\det L > 0$.

In the present work, we use the spherical coordinate (θ, ϕ) to describe the magnetization vector, i.e., $\hat{\boldsymbol{m}} = (\sin\theta\cos\phi, \sin\theta\sin\phi, \cos\theta)$. As for the linear analysis of two singular points $\hat{\boldsymbol{m}}_N = (0,0,1)$ and $\hat{\boldsymbol{m}}_S = (0,0,-1)$, we use the Cartesian coordinate instead.

III. PHASE DIAGRAMS BY LINEAR ANALYSIS

In the following, we consider three cases for the direction of the spin polarization of the current, where (A) $\hat{\boldsymbol{m}}_{\rm pin} = \hat{\boldsymbol{e}}_z$, (B) $\hat{\boldsymbol{m}}_{\rm pin} = \hat{\boldsymbol{e}}_y$, and (C) $\hat{\boldsymbol{m}}_{\rm pin} = \hat{\boldsymbol{e}}_x$. In each case, the directions of the easy axis and of the magnetic field, both of which lie in the film plane, are assumed to be (a) parallel or (b) perpendicular to each other. In summary, we consider $3 \times 2 = 6$ configurations of the three directions; the spin polarization of the current, the easy axis of the free layer, and the magnetic field. Here, the coordinate axes are taken so that the x axis is perpendicular to the film plane, i.e., $\hat{\boldsymbol{e}}_x = \hat{\boldsymbol{n}}$, and the z axis is parallel to the magnetic field, i.e., $\boldsymbol{H}_{\rm ext} = H_{\rm ext}\hat{\boldsymbol{e}}_z$. The direction of the easy axis $\hat{\boldsymbol{c}}$ is equal to $\hat{\boldsymbol{e}}_z$ for case (a) and $\hat{\boldsymbol{e}}_y$ for case (b). Putting all cases together, the effective field $\tilde{h}_\perp$ is written as

$$\tilde{h}_\perp = \sum_{\xi=\theta,\phi} (\tilde{h}^0_\xi + \tilde{h}^j_\xi)\hat{\boldsymbol{e}}_\xi, \tag{8}$$

where

$$\tilde{h}^0_\theta = -(\lambda \cos 2\phi + \mu)\sin\theta\cos\theta - h\sin\theta, \tag{9}$$

$$\tilde{h}^0_\phi = \lambda \sin 2\phi \sin\theta, \tag{10}$$

$$(\tilde{h}^j_\theta, \tilde{h}^j_\phi) = \begin{cases} (0, j\sin\theta) & \text{for (A)}, \\ (j\cos\phi, -j\cos\theta\sin\phi) & \text{for (B)}, \\ (-j\sin\phi, -j\cos\theta\cos\phi) & \text{for (C)}. \end{cases} \tag{11}$$

Here, we have introduced dimensionless parameters

$$(\lambda, \mu) \equiv \begin{cases} (1, 1+k) & \text{for (a)}, \\ (1+k/2, 1-k/2) & \text{for (b)}, \end{cases} \tag{12}$$

$$k \equiv H_K/2\pi M, \quad h \equiv H_{\rm ext}/2\pi M. \tag{13}$$

A. $\hat{\boldsymbol{m}}_{\rm pin} = \hat{\boldsymbol{e}}_z$ case

When $\hat{\boldsymbol{m}}_{\rm pin} = \hat{\boldsymbol{e}}_z$, two states corresponding to $\hat{\boldsymbol{m}}_N$ and $\hat{\boldsymbol{m}}_S$ are always equilibrium. They are stable when

$$j \gtrless -\alpha(h \pm \mu), \quad j^2 + (h \pm \mu)^2 > \lambda^2. \tag{14}$$

Here, $>$ and $+$ ($<$ and $-$) correspond to $\hat{\boldsymbol{m}}_N$ ($\hat{\boldsymbol{m}}_S$). Moreover, the states corresponding to $\hat{\boldsymbol{m}}_\pm = (\sin\theta_\pm\cos\phi_\pm, \sin\theta_\pm\sin\phi_\pm, \cos\theta_\pm)$ are also in equilibrium when $\theta_\pm \in (0, \pi)$ and $\phi_\pm \in [0, 2\pi)$ such that

$$\cos\theta_\pm = \frac{-h}{\mu \pm \sqrt{\lambda^2 - j^2}},$$

$$\cos 2\phi_\pm = \pm\sqrt{1 - j^2/\lambda^2}, \quad \sin 2\phi_\pm = -j/\lambda. \tag{15}$$

We notice that if a pair (θ, ϕ) satisfies Eq. (15), then $(\theta, \phi + \pi)$ also satisfies Eq. (15). We describe $\hat{\boldsymbol{m}}_+$ ($\hat{\boldsymbol{m}}_-$) as if it were one vector, but we must keep in mind that it actually corresponds to two vectors. The equilibrium state denoted by $\hat{\boldsymbol{m}}_+$ is stable when

$$|j| \leqslant \lambda, \quad |h| - \mu < \sqrt{\lambda^2 - j^2},$$

$$h^2 - \frac{2hj}{\alpha} > (\mu + \sqrt{\lambda^2 - j^2})(\mu + 3\sqrt{\lambda^2 - j^2}). \tag{16}$$

The equilibrium state denoted by $\hat{\boldsymbol{m}}_-$ is stable when

$$(|h| + \mu)^2 + j^2 < \lambda^2,$$

$$h^2 - \frac{2hj}{\alpha} < (\mu - \sqrt{\lambda^2 - j^2})(\mu - 3\sqrt{\lambda^2 - j^2}). \tag{17}$$

Summarizing the above discussion, we can construct phase diagrams which classify the types of stable states. Figure 1 illustrates the phase diagrams where the direction of the uniaxial anisotropy are parallel to the (a) z axis and (b) y

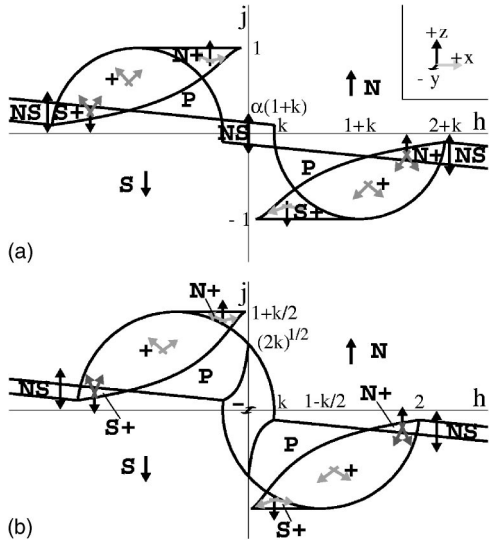

FIG. 1. Phase diagram of stable magnetization states for cases where $\hat{\boldsymbol{m}}_{\rm pin}=\hat{\boldsymbol{e}}_z$ and (a) $\hat{\boldsymbol{c}}=\hat{\boldsymbol{e}}_z$, (b) $\hat{\boldsymbol{c}}=\hat{\boldsymbol{e}}_y$. The dimensionless magnitude of the magnetization h and the current j are defined in Eqs. (13) and (5), respectively. The stable states vary continuously along paths inside a region surrounded by the boundary line, while they vary discontinuously along paths across the boundary line. The arrows denote the direction of the stable states for given h and j. They are depicted as projections to a plane which is slightly inclined against the (xz) plane. The dark arrow indicates that the magnetization points in the in-plane direction, while the light arrow indicates it points in the perpendicular-to-plane direction.

axis, respectively. The label of each regions in the phase diagram identifies the type of the stable states for the region. "NS," for instance, means that $\hat{\boldsymbol{m}}_N$ and $\hat{\boldsymbol{m}}_S$ are stable while $\hat{\boldsymbol{m}}_+$ and $\hat{\boldsymbol{m}}_-$ are unstable (or nonexistent). In the region "*P*," there are no stable states. We can see from the figure that any point in the whole (h,j) plane can be identified with one of seven types, namely, "*N*," "*S*," "NS," "+," "*N*+," "*S*+," "−," or "*P*."

The previously obtained phase diagrams in Refs. 12 and 14 are limited regions of our phase diagram in Fig. 1(a). What we have obtained covers the whole ranges of the current and the magnetic field. In our notation, the coercive force corresponds to $h_c=k$. The critical current[5,10,15] needed for the magnetization reversal by the spin-transfer torque is $j_c=\alpha(h\pm\mu)$. Our new findings are summarized as follows.

First, the regions +, *N*+, and *S*+, where the equilibrium state denoted by $\hat{\boldsymbol{m}}_+$ is stable, are revealed. A necessary condition is that j and h have opposite signs. The magnetization prefers $\hat{\boldsymbol{m}}_N$ in the case where $j>0$ and $h=0$, while it prefers $\hat{\boldsymbol{m}}_S$ in the case where $j=0$ and $h<0$. Thus, the opposite signs of j and h implies the competition of the two torques. It is worth noting that the direction $\hat{\boldsymbol{m}}_+$ is almost perpendicular to the plane, which is noncollinear to both the spin-polarization of the current and the magnetic field.

Second, the region *P*, where stable equilibrium states are nonexistent, is also revealed. The magnetization never stop rotating in this region. Such a nonrelaxing phenomenon is characteristic to systems where energy is fed from the outside. The linear analysis cannot predict the details of this dynamic behaviors in nonlinear regimes. We discuss this problem in the next section.

Third, the difference between (a) and (b) is clear when both h and j are comparably small. The applied magnetic field is parallel to the easy axis in the former case, while it is parallel to the hard axis in the latter case. When the field $H_{\rm ext}(<H_K)$ parallel to the hard axis is applied, it is known that the magnetization orients to the intermediate direction. This stable state corresponds to $\hat{\boldsymbol{m}}_-$ in our notation. We see that this state is extended to finite current region in the case (b), while it never appears in the case (a).

B. $\hat{\boldsymbol{m}}_{\rm pin}=\hat{\boldsymbol{e}}_y$ case

When $\hat{\boldsymbol{m}}_{\rm pin}=\hat{\boldsymbol{e}}_y$, the stable equilibrium states are classified into one of three types

$$(N):(\lambda+\mu)\sin\theta\cos\theta+h\sin\theta-|j|=0,\ \cos\phi=\mathrm{sgn}(j),$$

$$(S):(\lambda+\mu)\sin\theta\cos\theta+h\sin\theta+|j|=0,\ \cos\phi=-\mathrm{sgn}(j),$$

$$(J):\cos\theta=\frac{h}{\dfrac{j^2}{2\lambda}+\lambda-\mu},\ \cos\phi=\frac{j}{2\lambda}\frac{h}{\sqrt{\left(\dfrac{j^2}{2\lambda}+\lambda-\mu\right)^2-h^2}}. \tag{18}$$

The solution $(N)[(S)]$ is a state which is a extension of $\hat{\boldsymbol{m}}_N(\hat{\boldsymbol{m}}_S)$ for nonzero j. Namely, it is a state where the torque by the field is dominant over that by the current. On the other hand, the torque by the current is dominant over that by the field in the state (J). The direction approaches $\pm\hat{\boldsymbol{m}}_{\rm pin}$ as $h\to 0$ for the state.

The results of the linear stability analysis are summarized as phase diagrams in Fig. 2 for the case where (a) $\hat{\boldsymbol{c}}=\hat{\boldsymbol{e}}_z$, (b) $\hat{\boldsymbol{c}}=\hat{\boldsymbol{e}}_y$. We find that state (N) [or (S)] and the state (J) never become stable simultaneously. We also notice that the nonexistence of the region *P*, which means that at least one stable equilibrium state always exists for this case.

C. $\hat{\boldsymbol{m}}_{\rm pin}=\hat{\boldsymbol{e}}_x$ case

When $\hat{\boldsymbol{m}}_{\rm pin}=\hat{\boldsymbol{e}}_x$, the stable equilibrium states are classified into one of the three states

$$(N):(-\lambda+\mu)\sin\theta\cos\theta+h\sin\theta-|j|=0,\ \sin\phi=-\mathrm{sgn}(j),$$

$$(S):(-\lambda+\mu)\sin\theta\cos\theta+h\sin\theta+|j|=0,\ \sin\phi=\mathrm{sgn}(j),$$

$$(J):\cos\theta=\frac{-h}{\dfrac{j^2}{2\lambda}+\lambda+\mu},\ \cos\phi=\frac{-j}{2\lambda}\frac{h}{\sqrt{\left(\dfrac{j^2}{2\lambda}+\lambda+\mu\right)^2-h^2}}. \tag{19}$$

Again, the torque by the field is dominant for the states (N) and (S), while the torque by the current is dominant for the state (J).

The results of the linear stability analysis is summarized

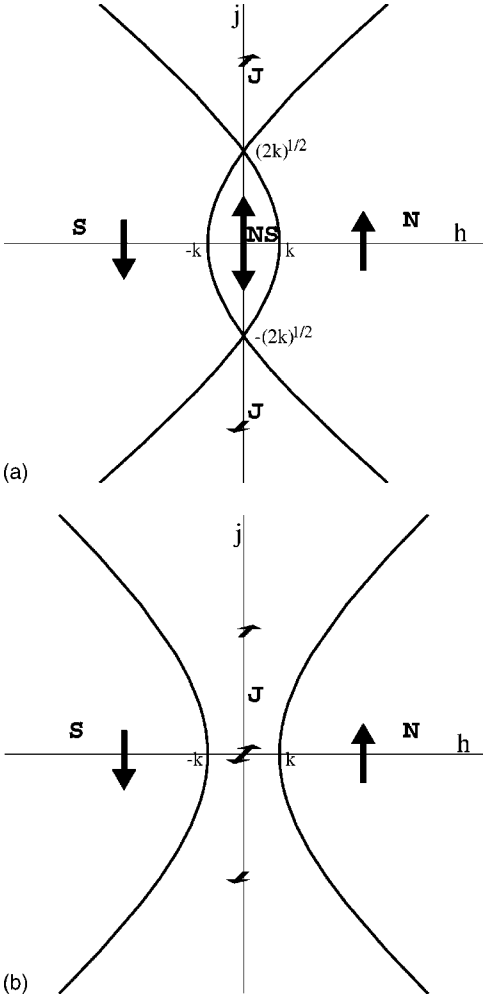

FIG. 2. Phase diagram of stable equilibrium states for the case where $\hat{\boldsymbol{m}}_{\text{pin}}=\hat{\boldsymbol{e}}_y$ and (a) $\hat{\boldsymbol{c}}=\hat{\boldsymbol{e}}_z$, (b) $\hat{\boldsymbol{c}}=\hat{\boldsymbol{e}}_y$.

as phase diagrams in Fig. 3 for the case where (a) $\hat{\boldsymbol{c}}=\hat{\boldsymbol{e}}_z$ and (b) $\hat{\boldsymbol{c}}=\hat{\boldsymbol{e}}_y$. The region P appears if $k/2<\alpha(2+k/2)$.

IV. DYNAMIC BEHAVIORS

In this section, we focus on the system where both the spin-polarization of the current and the magnetic field are parallel to the easy axis of the free layer, i.e., $\hat{\boldsymbol{c}}=\hat{\boldsymbol{m}}_{\text{pin}}=\hat{\boldsymbol{e}}_z$. We consider Co/Cu/Co system as an example. The Gilbert constant, the saturation magnetization, and the axial anisotropy field are taken as $\alpha=0.014$, $4\pi M=10$ kOe, and $H_K=500$ Oe, respectively.[14] The phase diagram in Fig. 1(a) is redrawn in Fig. 4(a), which is an extended phase diagram compared with the figure in Ref. 14. We pick up the three points A, B, and C in the phase diagram to elucidate relevant properties of the magnetization dynamics, which are ignored in the previous works. Among the three points, the points B and C lie outside the diagram in Ref. 14.

Point A lies in the region P, where no stable equilibrium states exist. Figure 4(b) illustrates a typical trajectory of the magnetization vector for this case. We find that the trajectory of the motion of the vector forms a closed path. This fact is not an accident but a logical consequence of Poincaré-Bendixson theorem in the dynamical systems theory.[16] Namely, the system we are dealing with does not have enough freedoms to cause chaotic dynamic behaviors. The closed-path is so-called "limit cycle." This periodic motion is observed as the precessional motion of the magnetization.

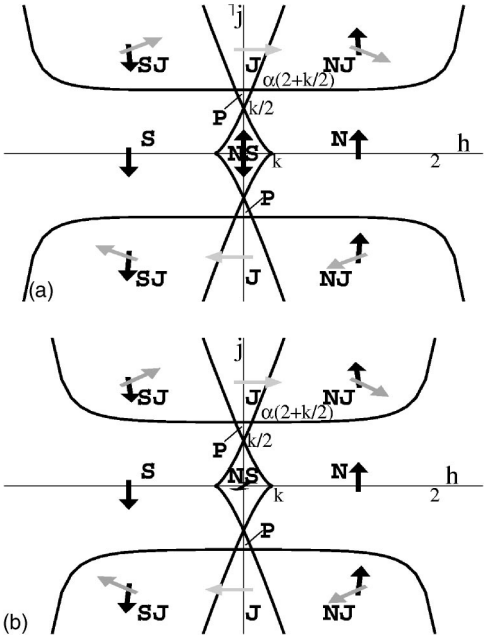

FIG. 3. Phase diagram of stable states for the case where $\hat{\boldsymbol{m}}_{\text{pin}}=\hat{\boldsymbol{e}}_x$ and (a) $\hat{\boldsymbol{c}}=\hat{\boldsymbol{e}}_z$, (b) $\hat{\boldsymbol{c}}=\hat{\boldsymbol{e}}_y$.

At point B, lying in the region S, there is one stable equilibrium state, $\hat{\boldsymbol{m}}_S$. However, it does not necessarily mean that the magnetization eventually orient to $\hat{\boldsymbol{m}}_S$. The trajectory in Fig. 4(c) illustrates such an example. In this case, the motion of the magnetization exhibit precessional motion if an appropriate initial condition is chosen. In other words, the precessional motion is possible outside the region P in the phase diagram. The region P indicates only a sufficient condition for the precessional motion.

At the point C, lying in the region $S+$, there are three stable equilibrium states $\hat{\boldsymbol{m}}_S$ and two $\hat{\boldsymbol{m}}_+$'s. The equilibrium state which the magnetization finally obtains depends on the initial condition. Figure 4(d) illustrates an example where the magnetization finally orients to $\hat{\boldsymbol{m}}_+$, which is nearly perpendicular to the plane.

Applying the values of the known critical current density[14] $J_c=3\times10^7$ A/cm^2 and the anisotropy field $H_K=500$ Oe, we notice that the point C corresponds to the case where $J\sim10^9$ A/cm^2 and $H_{\text{ext}}\sim5$ kOe. To observe a nontrivial equilibrium state such as $\hat{\boldsymbol{m}}_+$, a rather larger current density is required than that used in current experiments.

V. CONCLUSIONS

The magnetization receives torques from a spin-polarized current and a magnetic field independently. We have studied exhaustively the stable states of the magnetization under such circumstances, employing the macrospin model with the LLG equation. We have revealed all the possible stable

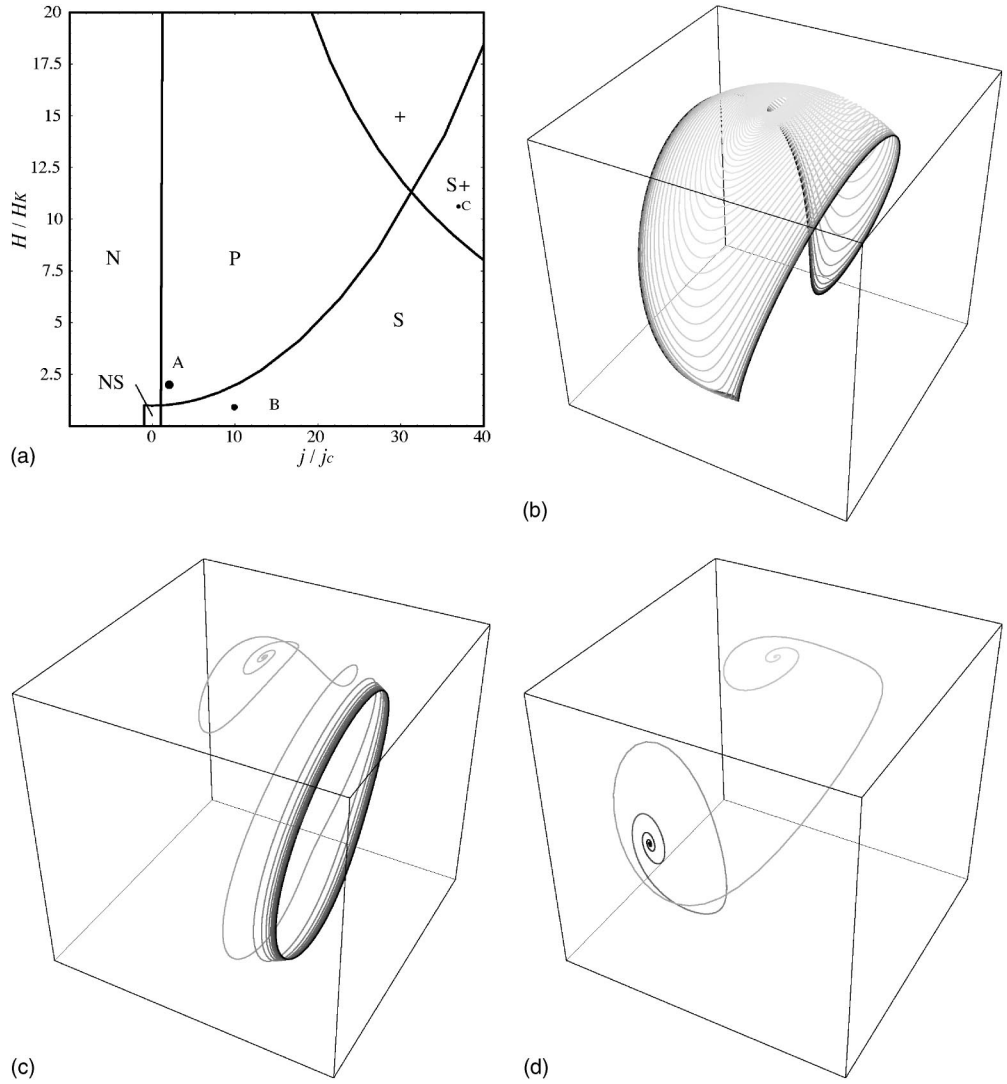

FIG. 4. (a) The phase diagram for the case where $\hat{\boldsymbol{m}}_{\mathrm{pin}}=\hat{\boldsymbol{c}}=\hat{\boldsymbol{e}}_z$. The units of the current j and the magnetic field H_{ext} are taken as $j_c=\alpha$ (the critical current) and H_K, respectively. (b)–(d) Typical trajectories of the magnetization motion for the points A–C in the phase diagram (a). The darkness of the point on the trajectory gradually increases with time. The black line or point indicates the final state.

states in the whole current-field plane including the regions which have not been investigated previously. We constructed six phase diagrams corresponding to different configurations for the combination of the three directions, that is, the easy axis of the magnet, the spin polarization of the current, and the magnetic field.

When either a spin-polarized current or a magnetic field is introduced, the orientations of the magnetization must be collinear to the spin polarization of the current or the magnetic field, respectively. On the other hand, other possibilities arise when both of them are introduced simultaneously. In some cases, a noncollinear equilibrium state becomes stable. In other cases, the magnetization does not stop rotation and it converges to a stable precessional motion. Such a nonequilibrium state is owing to the continuous energy injection fed by the current. Moreover, the motion of the magnetization is proved to be periodic if it does not converge to a fixed direction. In other words, the system we are dealing with does not have enough freedoms to cause chaotic dynamic behaviors. Nevertheless, the initial condition has a significant effect on the motion of the magnetization. The magnetization motion converges to a fixed direction for an initial condition, while it converges to a precessional motion for another condition. Namely, the condition that no stable equilibrium states exist yields only a sufficient condition for such a precessional motion.

To observe nontrivial stable magnetization states in experiments, a comparably large current is necessary. When one uses cobalt as the magnetic layers, a current density of at least the order of 10^8-10^9 A/cm^2 is required. However, this required current density will be reduced if the efficiency of the spin-transfer torque is improved by use of highly spin-polarized magnetic materials, such as half metals.

Finally, it is possible to extend the present work based on the macrospin model to the micromagnetic simulation. In particular, it is worth investigating the dynamic behavior of the microscopic structure of the magnetization under the competitive torques by a spin-polarized current and a mag-

netic field. In Ref. 17, the chaotic magnetization motion induced by the spin transfer torque is studied. It indicates to us that the nontrivial dynamic behavior of the magnetization is remarkable when the inhomogeneity of the magnetization is taken into consideration.

ACKNOWLEDGMENT

The authors wish to thank Dr. S. Haneda for stimulating discussions.

*Electronic address: hirofumi.morise@toshiba.co.jp

[1] J. C. Slonczewski, J. Magn. Magn. Mater. **159**, L1 (1996).
[2] L. Berger, Phys. Rev. B **54**, 9353 (1996).
[3] E. B. Myers, D. C. Ralph, J. A. Katine, R. N. Louie, and R. A. Buhrman, Science **285**, 867 (1999).
[4] M. Tsoi, A. G. M. Jansen, J. Bass, W.-C. Chiang, M. Seck, V. Tsoi, and P. Wyder, Phys. Rev. Lett. **80**, 4281 (1998).
[5] J. A. Katine, F. J. Albert, R. A. Buhrman, E. B. Myers, and D. C. Ralph, Phys. Rev. Lett. **84**, 3149 (2000).
[6] F. J. Albert, J. A. Katine, R. A. Buhrman, and D. C. Ralph, Appl. Phys. Lett. **77**, 3809 (2000).
[7] E. B. Myers, F. J. Albert, J. C. Sankey, E. Bonet, R. A. Buhrman, and D. C. Ralph, Phys. Rev. Lett. **89**, 196801 (2002).
[8] J. Grollier, V. Cros, A. Hamzic, J. M. George, H. Jaffrès, A. Fert, G. Faini, J. B. Youssef, and H. Legall, Appl. Phys. Lett. **78**, 3663 (2001).
[9] J. Z. Sun, D. J. Monsma, D. W. Abraham, M. J. Rooks, and R. H. Koch, Appl. Phys. Lett. **81**, 2202 (2002).
[10] J. Z. Sun, Phys. Rev. B **62**, 570 (2000).
[11] Z. Li and S. Zhang, Phys. Rev. B **68**, 024404 (2003).
[12] J. Grollier, V. Cros, H. Jaffrès, A. Hamzic, J. M. George, G. Faini, J. B. Youssef, H. LeGall, and A. Fert, Phys. Rev. B **67**, 174402 (2003).
[13] Y. B. Bazaliy, B. A. Jones, and S. C. Zhang, J. Appl. Phys. **89**, 6793 (2001).
[14] S. I. Kiselev, J. C. Sankey, I. N. Krivorotov, N. C. Emley, R. J. Schoelkopf, R. A. Buhrman, and D. C. Ralph, Nature (London) **425**, 380 (2003).
[15] J. C. Slonczewski, J. Magn. Magn. Mater. **195**, L261 (1999).
[16] M. W. Hirsch and S. Smale, *Differential Equations, Dynamical Systems, and Linear Algebra* (Academic Press, New York, 1974).
[17] X. Zhu, J.-G. Zhu, and R. M. White, J. Appl. Phys. **95**, 6630 (2004).